THE JOURNAL OF BIOLOGICAL CHEMISTRY VOL. 283, NO. 47, pp. 32691–32703, November 21, 2008

The Nociceptor Ion Channel TRPA1 Is Potentiated and Inactivated by Permeating Calcium Ions*[S]

Received for publication, May 9, 2008, and in revised form, September 4, 2008 Published, JBC Papers in Press, September 5, 2008, DOI 10.1074/jbc.M803568200

Yuanyuan Y. Wang[‡§], Rui B. Chang[‡§], Hang N. Waters[‡], David D. McKemy[‡§], and Emily R. Liman[‡§1]

From the Department of Biological Sciences, [‡]Section of Neurobiology and [§]Program in Neuroscience, University of Southern California, Los Angeles, California 90089

The transient receptor potential A1 (TRPA1) channel is the molecular target for environmental irritants and pungent chemicals, such as cinnamaldehyde and mustard oil. Extracellular Ca^{2+} is a key regulator of TRPA1 activity, both potentiating and subsequently inactivating it. In this report, we provide evidence that the effect of extracellular Ca^{2+} on these processes is indirect and can be entirely attributed to entry through TRPA1 and subsequent elevation of intracellular calcium. Specifically, we found that in a pore mutant of TRPA1, D918A, in which Ca^{2+} permeability was greatly reduced, extracellular Ca^{2+} produced neither potentiation nor inactivation. Both processes were restored by reducing intracellular Ca^{2+} buffering, which allowed intracellular Ca^{2+} levels to become elevated upon entry through D918A channels. Application of Ca^{2+} to the cytosolic face of excised patches was sufficient to produce both potentiation and inactivation of TRPA1 channels. Moreover, in whole cell recordings, elevation of intracellular Ca^{2+} by UV uncaging of 1-(4,5-dimethoxy-2-nitrophenyl)-EDTA-potentiated TRPA1 currents. In addition, our data show that potentiation and inactivation are independent processes. TRPA1 currents could be inactivated by Mg^{2+}, Ba^{2+}, and Ca^{2+} but potentiated only by Ba^{2+} and Ca^{2+}. Saturating activation by cinnamaldehyde or mustard oil occluded potentiation but did not interfere with inactivation. Last, neither process was affected by mutation of a putative intracellular Ca^{2+}-binding EF-hand motif. In conclusion, we have further clarified the mechanisms of potentiation and inactivation of TRPA1 using the D918A pore mutant, an important tool for investigating the contribution of Ca^{2+} influx through TRPA1 to nociceptive signaling.

Members of the transient receptor potential (TRP)[2] family of ion channels that are expressed by sensory neurons in dorsal root and trigeminal ganglia serve as sensors for temperature and noxious stimuli (1, 2). Of these, TRPA1 is one of the key sensors for pungent chemicals and environmental irritants and is essential for behavioral responses of mice to conditions that evoke inflammatory pain (3–7). Inflammatory mediators, such as bradykinin, bind to G protein-coupled receptors on nociceptors, initiating a second messenger signaling cascade that leads to Ca^{2+} influx mediated in part by the opening of Ca^{2+}-permeable TRPA1 channels (5, 8, 9). TRPA1 is also activated directly by a wide range of chemicals that cause painful sensations, including food additives, such as mustard oil (MO), cinnamaldehyde (Cin), onion, raw garlic, and thyme; environmental irritants, such as formaldehyde and acrolein (a component of automobile exhaust); and products of oxidative stress (4, 8, 10–16). Many of these chemicals activate TRPA1 by binding covalently to reactive cysteine residues in the amino terminus of the protein (17, 18), producing a modification of the channel that can last for more than 1 h and which leads to persistent activation of TRPA1 currents (18, 19).

Ca^{2+} plays at least two roles in regulating the activity of TRPA1 channels. TRPA1 currents that are activated by pungent chemicals are rapidly potentiated in the presence of extracellular Ca^{2+}, an effect that may be mediated by Ca^{2} entry through TRPA1 (4, 20, 21). This mechanism is attractive, since it could also account for the observed activation of TRPA1 by some inflammatory mediators (5, 8). For example, bradykinin, acting through its cognate receptor, stimulates a phospholipase C-based signaling pathway, leading to elevation of intracellular Ca^{2+}, and it has been proposed that Ca^{2+} is the proximate stimulus that gates TRPA1 (4, 5) (but see also Refs. 8 and 22). Activation of TRPA1 by intracellular Ca^{2+} has been observed in experiments where Ca^{2+} is dialyzed into cells or applied to excised patches (20, 21, 23), although it is not known whether this is the mechanism for Ca^{2+} potentiation or receptor activation of TRPA1. The site for Ca^{2+} activation of TRPA1 has been proposed to be an EF-hand present in the N terminus of the protein (20, 21).

A second and equally important effect of extracellular Ca^{2+} is to inactivate TRPA1 (*e.g.* see Refs. 4, 19, 20, and 24, but see also Ref. 19). TRPA1 currents activated by pungent chemicals in the absence of extracellular Ca^{2+}, decay within seconds when extracellular Ca^{2+} is introduced (24). Inactivation may be mediated by binding of Ca^{2+} to the outside of the channel or could be mediated by elevation of intracellular Ca^{2+}, which is known to cause desensitization of other TRP channels (25–31). Alternatively, inactivation of TRPA1 might simply reflect the stochastic and obligatory entry of the channel into the inacti-

* This work was supported, in whole or in part, by National Institutes of Health, NIDCD, Grant 004564 (to E. L.). The costs of publication of this article were defrayed in part by the payment of page charges. This article must therefore be hereby marked "*advertisement*" in accordance with 18 U.S.C. Section 1734 solely to indicate this fact.

[S] The on-line version of this article (available at http://www.jbc.org) contains supplemental Figs. 1–7.

[1] To whom correspondence should be addressed: Section of Neurobiology, University of Southern California, 3641 Watt Way, Los Angeles, CA 90089-2520. Tel.: 213-821-1454; Fax: 213-821-5290; E-mail: Liman@usc.edu.

[2] The abbreviations used are: TRP, transient receptor potential; TRPA1, transient receptor potential A1; Cin, cinnamaldehyde; MO, mustard oil; $PI(4,5)P_2$, phosphatidylinositol 4,5-bisphosphate; YFP, yellow fluorescent protein; rTRPA1, rat TRPA1; hTRPA1, human TRPA1; $polyP_3$, pentasodium tripolyphosphate hexahydrate; DMNP, 1-(4,5-dimethoxy-2-nitrophenyl); pS, picosiemens; WT, wild type.

vated state, following Ca^{2+}-dependent activation, similar to inactivation of voltage-gated ion channels (32).

By studying mutant TRPA1 channels in which Ca^{2+} permeability is reduced, we show that both the potentiating and inactivating effects of extracellular Ca^{2+} can be attributed to entry of Ca^{2+} through TRPA1 and the subsequent elevation of intracellular Ca^{2+}. We also provide evidence that potentiation and inactivation are mediated by independent mechanisms, each with a distinct sensitivity and specificity for divalent cations.

EXPERIMENTAL PROCEDURES

cDNAs and Expression in HEK-293 Cells—For most experiments, we used an N-terminal YFP fusion of rat TRPA1 generated by inserting a PCR fragment of YFP into an AgeI site at the 5′-end of a rat TRPA cDNA. To confirm that the YFP fusion did not alter function, in some experiments we used an unaltered clone of rTRPA1, which was co-transfected with green fluorescent protein (20:1). To assess whether some of our results could be attributed to species differences between rat and human variants of TRPA1, in some experiments, we used hTRPA1, co-expressed at a ratio of 20:1 with green fluorescent protein. Point mutations were generated by QuikChange mutagenesis (Stratagene, La Jolla, CA) and were verified by sequencing (Retrogen (San Diego, CA) or Macrogen (Rockville, MD)). All constructs were transiently transfected into HEK-293 cells using TransIT®-LT1 (Mirus Bio Corp., Madison, WI), as suggested by the manufacturer, and cells were cultured at 37 °C. Prior to recording, cells were treated with 0.05% trypsin and 4 mM EDTA in phosphate-buffered saline for 5 min at 37 °C and replated in the recording chamber with Tyrode's solution. Transfected cells were identified under epifluorescence. Recordings were performed ~24–48 h after transfection at room temperature.

Patch Clamp Recording—Patch clamp electrophysiology was performed as previously described (27, 33). In brief, recordings were made with an Axopatch 200B amplifier, sampled at 5 kHz, and filtered at 1 kHz. Data were digitized with a Digidata 1322a digitizer, acquired with pClamp 8.2, and analyzed with Clampfit 8.2 (Axon Instruments, Union City, CA). Representative data shown in figures were exported into Origin (Microcal, Northampton, MA) and CorelDRAW (Corel Corp., Eden Prairie, MN). Pipettes were fabricated from borosilicate glass, fire-polished to a resistance of 2–3 megaohms. For whole-cell recordings, the membrane potential was ramped from −80 mV to +80 mV (1 V/s). Excised patch recording was performed as previously described (27). Briefly, following formation of a gigaohm seal, the patch was excised into Ca^{2+}-free solution and rapidly moved in front of a linear array of microperfusion pipes (Warner Instruments, Hamden, CT).

Solutions—Tyrode's solution contained 145 mM NaCl, 5 mM KCl, 1 mM $MgCl_2$, 2 mM $CaCl_2$, 20 mM dextrose, 10 mM HEPES (pH 7.4 with NaOH). Ca^{2+}-free bath solution was as follows: 150 mM NaCl, 10 mM HEPES, 2 mM HEDTA. Ca^{2+}-, Mg^{2+}-, or Ba^{2+}-containing bath solutions contained 150 mM NaCl, 10 mM HEPES (pH 7.4 with NaOH), and 200 μM, 2 mM, or 10 mM $CaCl_2$, 2 mM Mg^{2+}, or 2 mM Ba^{2+}. For lower Ca^{2+} concentrations, 1.5 mM Ca^{2+} or 1.9 mM Ca^{2+} was added to Ca^{2+}-free solution buffered by 2 mM HEDTA, to produce 12 or 50 μM free Ca^{2+}, respectively. Low buffer internal Cs^+-based solution (LB-Cs^+) contained 0.02 mM EGTA, 145 mM CsCl, 2 mM MgATP, 10 mM HEPES, and high buffer internal Cs^+-based solution (HB-Cs^+) contained 5 mM EGTA, 3 mM $CaCl_2$ (100 nM free Ca^{2+}), 145 mM CsCl, 2 mM MgATP, 10 mM HEPES (pH 7.4 with CsOH). For excised inside-out patch experiments, the pipette solution contained 150 mM NaCl, 10 mM HEPES with either 2 mM EGTA or 2 mM HEDTA (pH 7.4). Ca^{2+}-free solution contained 150 mM NaCl, 10 mM HEPES, with either 2 mM EGTA or 2 mM HEDTA. Cytosolic solutions with nanomolar or micromolar concentrations of free Ca^{2+} were obtained by adding Ca^{2+} (1.22, 1.65, 1.77, 1.88, or 1.98 mM) to Ca^{2+}-free solution buffered by 2 mM EGTA to obtain free Ca^{2+} concentrations of 100 nM, 300 nM, 500 nM, 1 μM, and 5.2 μM, respectively. 1 mM pentasodium tripolyphosphate hexahydrate (polyP_3) was added to the cytoplasmic solution for excised patch experiments. All Ca^{2+} concentrations are reported as calculated with MaxChelator (available on the World Wide Web). For cell-attached recordings, bath KCl was substituted for NaCl to zero the membrane potential. For flash photolysis experiments, caged Ca^{2+} solution contained 120 mM cesium aspartate, 20 mM CsCl, 10 mM HEPES, 2.5 mM 2,6-dimethyl-4-nitropyridine-EDTA (DMNP-EDTA; Invitrogen), 0.75 mM $CaCl_2$, pH 7.4. The bath solution in ion permeability experiments contained NaCl, KCl, CsCl, or N-methyl-D-glucamine chloride (150 mM), 10 mM HEPES, and 2 mM HEDTA, or $CaCl_2$ (128 mM) with 10 mM HEPES (pH 7.4 with NaOH). For recordings during which intracellular Ca^{2+} concentration was measured, the pipette solution contained 20 μM Fura-4F, 145 mM CsCl, 2 mM MgATP, 10 mM HEPES, with or without 5 mM EGTA, or 10 μM Fluo-5F in caged Ca^{2+} solution (with 2 mM MgATP and 3 mM Na_2ATP).

Flash Photolysis of Caged Compound—All experiments were performed on an Olympus IX71 microscope. To allow uniform dialysis of the cell with the caged compounds, we waited at least 100 s after breaking into whole cell recording mode before uncaging. UV light from a mercury arc lamp that was then passed through a ×350/50 band pass filter (Chroma Technology Corp., Rockingham, VT) was controlled by a Uniblitz shutter (Vincent Associates, Rochester, NY). The shutter was opened for 100 ms to uncage Ca^{2+}. For experiments in which Ca^{2+} levels were measured, UV light from a xenon arc lamp was passed through a band pass filter (380xv1; Chroma Technology) that was part of a Ludl Electronic Products (Hawthorne, NY) filter wheel/shutter operated under computer control (Simple PCI; Compix Corp., Sewickley, PA). The shutter was opened for 1 s to uncage Ca^{2+}.

Ca^{2+} Imaging—Ca^{2+} imaging was performed as previously described (33). Images were acquired on an Olympus IX71 microscope equipped with a Ludl Electronic Products filter wheel and ORCA ER camera (Hamamatsu Photonics) and were analyzed with simple PCI (Compix Corp.). The low affinity Ca^{2+} indicator Fluo-5F (10 μM) or Fura-4F (20 μM) was loaded through the patch pipette. The fluorescence emission from Fluo-5F was detected using a YFP filter set (Chroma Technology). The fluorescence emission from Fura-4F was detected with a Fura 2 filter set (Chroma Technology) using excitation alternately at 340 and 380 nM. The ratio of the fluorescence

emission ($r = F_{340}/F_{380}$) was used to calculate the intracellular Ca^{2+} concentration as follows,

$$[Ca^{2+}]_i = K_d \times Q \times \frac{(R - R_{min})}{(R_{max} - R)} \quad \text{(Eq. 1)}$$

where K_d is the Ca^{2+} dissociation constant of the indicator Fura-4F (770 nM), Q is emission ratio at 380 nM recorded at 0 Ca^{2+} and at a saturated Ca^{2+} concentration, and R_{max} and R_{min} are the ratios under saturating Ca^{2+} or 0 Ca^{2+} conditions, respectively. R_{min} was measured from a separate set of cells in which intracellular solution was heavily buffered by 5 mM EGTA, and the extracellular solution was Ca^{2+}-free (buffered with 2 mM HEDTA). To obtain R_{max} and Q, at the end of each experiment, ionomycin was added to the bath, and the emission with 2 mM Ca^{2+} and 0 Ca^{2+} in the bath was measured.

Ion Selectivity Measurements—TRPA1 currents were activated by brief exposure to Cin, and the current in the presence of different external cations was measured by rapidly exchanging the extracellular solution using a linear array of microperfusion pipes. The internal solution contained Cs^+ (HB-Cs^+), and the ion permeability relative to Cs^+ was calculated from the reversal potential under bi-ionic conditions according to Equations 2 and 3,

$$\frac{P_{Ca}}{P_{Cs}} = \frac{[Cs^+]_i}{4[Ca^{2+}]_o} \times \exp\left(E_{rev} \times \frac{F}{RT}\right) \times \left(\exp\left(E_{rev} \times \frac{F}{RT}\right) + 1\right) \quad \text{(Eq. 2)}$$

$$\frac{P_X}{P_{Cs}} = \exp\left(E_{rev} \times \frac{F}{RT}\right) \quad \text{(Eq. 3)}$$

where P_{Ca}/P_{Cs} and P_X/P_{Cs} are the Ca^{2+} and monovalent cation permeability relative to Cs^+, respectively, E_{rev} is the reversal potential, F is Faraday's constant, R is the universal gas constant, and T is the absolute temperature (34). E_{rev} was corrected for the liquid junction potentials measured under the conditions of our experiments.

Chemicals—Cinnamaldehyde, menthol, mustard oil, and $polyP_3$ were purchased from Sigma. Fluo-5F, Fura-4F, and ionomycin were from Invitrogen Molecular probes (Eugene, OR). HC-030031 was from ChemBridge (San Diego, CA). For stock solutions, Cin, HC-030031, mustard oil, and ionomycin were dissolved in dimethyl sulfoxide, menthol was in ethanol, and other chemicals were in water. Prior to use, the stock solution was diluted in the appropriate bath solution. The final dimethyl sulfoxide or ethanol concentration was <0.2%.

RESULTS

A Dual Effect of Extracellular Ca^{2+}; Potentiation and Inactivation of TRPA1—To study Ca^{2+} regulation of TRPA1 channels, we expressed rTRPA1 fused to YFP in HEK 293 cells and recorded responses to TRPA1 agonists with patch clamp electrophysiology. Bath perfusion of Cin (100 μM) for ~40 s in the absence of extracellular Ca^{2+} strongly activated a nonselective cation current of 3.9 ± 0.4 nA at +80 mV ($n = 10$) in TRPA1-expressing cells (Fig. 1*A*) but not in untransfected cells. The TRPA1 current persisted following washout of the agonist (Fig. 1*A*), consistent with the observation that Cin binds covalently to cysteine residues in the N terminus of the channel, and therefore its binding is not readily reversible (17, 18). The addition of 2 mM Ca^{2+} to the bath caused a strong potentiation, which was followed by a rapid decay of the current, as previously noted (4, 24) (Fig. 1*A*). We quantitated the degree of potentiation by the -fold increase in the current after introduction of Ca^{2+}, where 1 indicates no increase and 2 indicates a doubling of the current. Note that this analysis underestimates the full degree of potentiation, which is partly masked by the concomitant process of inactivation. In these experiments, the addition of 2 mM Ca^{2+} potentiated the currents by 1.85 ± 0.06-fold at +80 mV and 3.98 ± 0.50-fold at −80 mV ($n = 10$). The greater potentiation of the currents at negative voltages reflects a decrease in the outward rectification of the currents (from 6.56 ± 0.79 to 3.58 ± 0.76, measured as the current at +80 mV divided by the current at −80 mV), as is commonly observed during strong activation of many TRP channels (35). The currents subsequently decayed to 50% of their peak value (T50) in 4.8 ± 0.5 s (measured at +80 mV; $n = 10$). Similar results were obtained with MO as the agonist, indicating that as previously noted, Ca^{2+} potentiation and inactivation are independent of the specific agonist used to activate TRPA1 (21). Ca^{2+} potentiation and inactivation appeared to be unaffected by fusion of YFP to the N terminus of TRPA1, since there was no difference in the degree of potentiation or rate of inactivation when an unfused rTRPA1 cDNA was used (2.52 ± 0.45-fold and 4.85 ± 1.29-fold potentiation at +80 and −80 mV, respectively; T50 = 4.7 ± 0.9 s, $n = 3$; see supplemental Fig. 1).

To confirm that the decay of TRPA1 currents upon the addition of external Ca^{2+} represents inactivation rather than a return to the resting state, we determined whether TRPA1 currents could be reactivated following exposure to external Ca^{2+}. For these experiments, we used a low concentration of menthol, which does not bind covalently to TRPA1 and can be used to repeatedly activate TRPA1 currents in the absence of external Ca^{2+} (36). Following activation of TRPA1 by menthol, the addition of external Ca^{2+} caused a rapid potentiation and subsequent decay of the current similar to that observed when the channels had been activated by Cin (Fig. 1*B*). Following decay of the current, no additional responses to menthol could be evoked for a period up to 20 min (Fig. 1*B*; $n = 5$). Thus, external Ca^{2+} promotes the entry of TRPA1 channels into a long lasting inactivated state.

Complete Activation of TRPA1 by Cin Occludes Ca^{2+} Potentiation—For both practical and theoretical reasons, it was important to understand whether extracellular Ca^{2+} and Cin act independently or in concert to regulate gating of TRPA1. Toward this end, we determined whether TRPA1 currents could be potentiated by Ca^{2+} when the currents had been maximally activated by Cin. Because Cin binds covalently to TRPA1, the fraction of channels activated by a fixed concentration of the agonist is expected to be sensitive to the duration of the exposure. Consistent with this prediction, we found that a prolonged exposure (156 ± 17 s) to 100 μM Cin in the absence of external Ca^{2+} activated an average current of 7.7 ± 1.1 nA (at +80 mV, $n = 4$), which was twice as large as the average current measured in response to an exposure of ~40 s (Fig. 1, *C* and *D*;

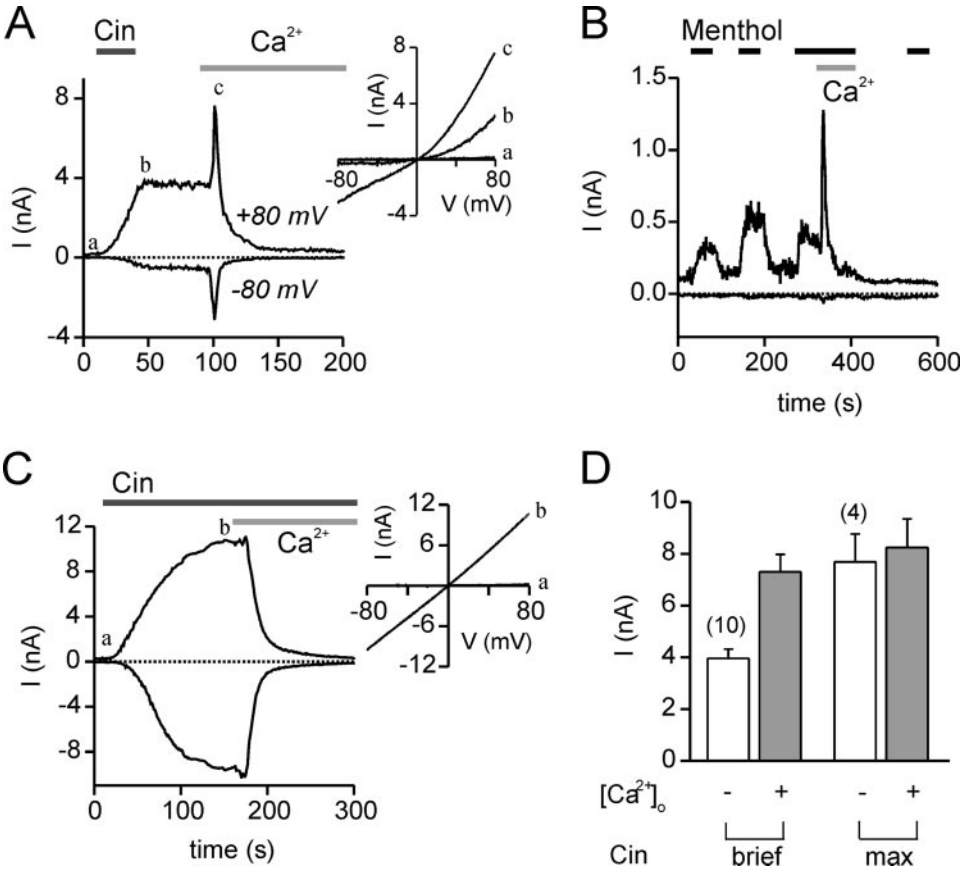

FIGURE 1. **TRPA1 channels are potentiated and inactivated by extracellular Ca^{2+}.** Currents were recorded from HEK-293 cells heterologously expressing an N-terminal YFP fusion of rat TRPA1. *A* and *B*, in the absence of extracellular Ca^{2+}, brief exposure to TRPA1 agonists, as indicated, elicited a current, which was first potentiated and then decayed to base line in response to the addition of extracellular Ca^{2+} (2 mM). *Inset*, the *I*-V relationship in response to a ramp depolarization (1 V/s) at the times indicated. Agonists were menthol (30 μM) or Cin (100 μM). Note that following the introduction of Ca^{2+}, no additional responses to menthol could be measured, indicating that the channels had entered a long lasting inactivated state. *C*, TRPA1 currents in response to prolonged exposure to Cin (100 μM) in the absence of extracellular Ca^{2+} reached a plateau after ~100 s. The addition of 2 mM Ca^{2+} did not cause further activation but still promoted rapid inactivation of the currents. *Inset*, the *I*-V relationship in response to a ramp depolarization (1 V/s) at the times indicated. Note the linearization of the *I*-V curve with strong activation. *D*, magnitude of the TRPA1 currents at +80 mV before and after the addition of 2 mM Ca^{2+} from experiments as in *A* and *C*. The Cin-evoked currents measured with the brief exposure protocol were ~50% of the maximal Cin-evoked currents, and only these subsaturating responses could be potentiated by Ca^{2+}.

see above). After exposure to Cin for ~120 s, the currents reached a plateau, presumably reflecting the full activation of TRPA1 channels (Fig. 1*C*). Interestingly, when fully activated, the currents were significantly less rectifying than when they were partially activated (Fig. 1*C*; rectification ratio was 1.32 ± 0.20; $n = 4$). At this point, the addition of extracellular Ca^{2+} only slightly potentiated the currents (Fig. 1, *C* and *D*; -fold increase in current was 1.07 ± 0.04 and 1.12 ± 0.05 at +80 and −80 mV, respectively, $n = 4$), whereas inactivation was slightly slowed (T50 = 10.5 ± 3.0 s; $p < 0.05$ compared with brief exposure). Therefore, Ca^{2+} potentiation and Cin activation are not independent and may share a final common mechanism (23). Similar results were obtained for MO activation of hTRPA1 (supplemental Fig. 6). In the following experiments, we took care to only partially activate the channels with Cin or MO, so that Ca^{2+} potentiation would not be occluded.

Potentiation and Inactivation of TRPA1 by Micromolar Concentrations of Extracellular Ca^{2+}—The dual effects of Ca^{2+} on TRPA1 currents could be explained by several different mechanisms. First, inactivation might reflect an obligatory and stochastic conformational change that follows Ca^{2+}-dependent activation, like some forms of inactivation of voltage-dependent ion channels (32). This "coupled" model predicts that potentiation and inactivation will show a similar sensitivity and specificity for Ca^{2+} and that conditions that promote potentiation will similarly promote inactivation. Alternately, potentiation and inactivation may be mediated by "independent" Ca^{2+}-dependent processes. This model predicts that inactivation could be separable from activation. For each of these two mechanisms, external Ca^{2+} could act by binding to a site on the outside of the channel, or it could enter the cell, through TRPA1 channels, to act internally.

To determine if the processes of Ca^{2+}-dependent potentiation and Ca^{2+}-dependent inactivation are independent, we tested if the two could be separated based on their sensitivity to extracellular Ca^{2+} or other divalent cations. Following Cin activation of TRPA1, we varied the concentration of external Ca^{2+} that was introduced into the bath. Surprisingly, potentiation of TRPA1 currents could be induced by a Ca^{2+} concentration as low as 12 μM, and at 50 μM Ca^{2+}, the magnitude of the response was saturated, although the response kinetics were slowed as compared with responses to 2 mM Ca^{2+} (Fig. 2, *A* and *C*, 1.26 ± 0.05-fold increase at 12 μM Ca^{2+}, $n = 4$; 2.22 ± 0.16-fold increase at 50 μM Ca^{2+}, $n = 4$). In contrast, the rate of inactivation varied with Ca^{2+} concentration over the entire range that we tested (12 μM to 10 mM) (Fig. 2, *A* and *D*). Importantly, at low Ca^{2+} concentrations that still induced maximal potentiation, (*e.g.* 50 μM), inactivation was substantially slower as compared with control conditions (2 mM Ca^{2+}), suggesting that inactivation does not derive its Ca^{2+} dependence from activation.

Potentiation and Inactivation of TRPA1 by Other Divalent Cations—In a similar series of experiments, we tested whether divalent cations other than Ca^{2+} could potentiate or inactivate TRPA1 currents. Introduction of Ba^{2+} (2 mM) produced both robust potentiation and rapid inactivation of TRPA1 currents (-fold increase of 1.83 ± 0.05; T50 of 12.0 ± 1.9 s; $n = 4$). In contrast, introduction of 2 mM Mg^{2+} caused little or no potentiation but significant inactivation (-fold increase of 1.13 ± 0.09; T50 of 47.5 ± 8.1 s; $n = 6$) (Fig. 2, *B–D*), and a higher

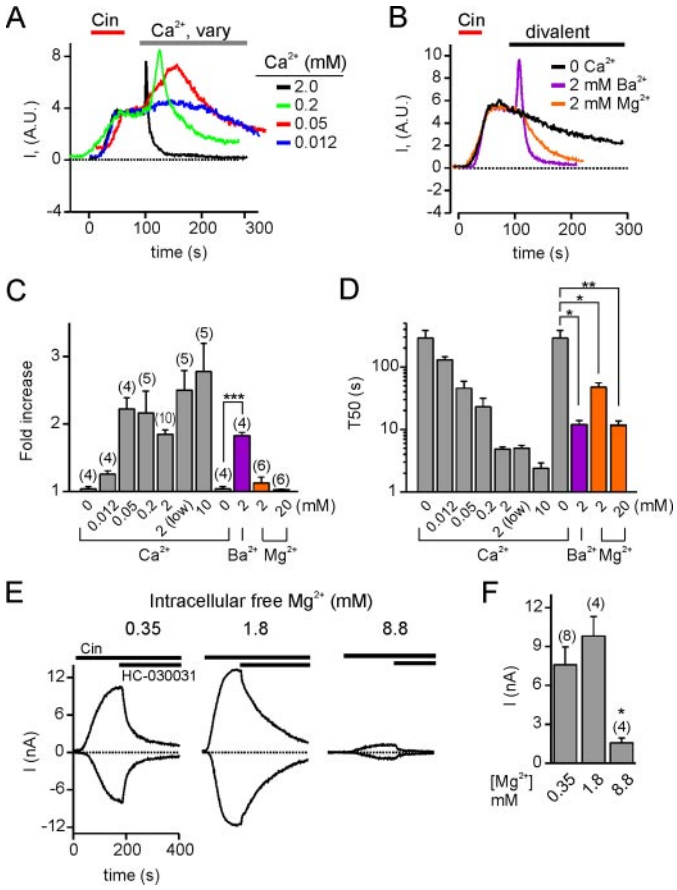

FIGURE 2. **Sensitivity and specificity of potentiation and inactivation of TRPA1.** *A*, TRPA1 currents evoked in response to brief exposure to Cin (100 μM) and the subsequent addition of varying concentrations of Ca^{2+} (as indicated). Note that each *trace* represents a recording from a separate cell, and the *traces* have been aligned by the time at which Ca^{2+} was introduced. The currents were scaled by the magnitude of the response to Cin, and therefore the *y* axis is represented by an arbitrary unit. *B*, currents evoked in response to brief exposure to Cin (100 μM) and the subsequent addition of Ba^{2+} or Mg^{2+} (2 mM). *C*, average data from experiments as in *A* and *B*. Potentiation was measured as the -fold increase in the current (at +80 mV) following the addition of the divalent cation, where *1* represents no change in the current. Note the "threshold" for potentiation of the current by extracellular Ca^{2+} was ~12 μM. The *bar* corresponding to the response to "0 Ca^{2+}" was duplicated to allow comparison with responses to Ba^{2+} and Mg^{2+}. *D*, inactivation was measured by the T50 or time, relative to the peak, at which the currents had decayed to 50% of their maximum value (at +80 mV). There was a continuous slowing of inactivation as the Ca^{2+} concentration was lowered. Data represent the mean ± S.E. (n = 4–10). Intracellular solution was HB-Cs^+ (which contained 5 mM EGTA) for *A* and *B*. *E*, TRPA1 currents elicited in response to a saturating exposure to Cin (100 μM) with varying concentrations of free Mg^{2+} in the pipette (as indicated). HC-030031 (10 μM) was introduced at the end of each experiment to confirm that the current was entirely due to the gating of TRPA1 channels. Intracellular solution was HB-Cs^+ with 0, 2, or 10 mM $MgCl_2$ added. *F*, magnitude of the current (+80 mV) from experiments as in *E*. Data represent the mean ± S.E. *, $p < 0.05$; **, $p < 0.01$; ***, $p < 0.001$.

concentration of Mg^{2+} (20 mM) promoted more rapid inactivation (T50 of 11.6 ± 2.2; -fold increase of 1.03 ± 0.01; n = 6; Fig. 2, *C* and *D*). Similar results were obtained using a clone of rTRPA1 that was not fused to YFP (see supplemental Fig. 1). We conclude that potentiation and inactivation are mediated by distinct processes that can be separated on the basis of their specificity for divalent cations.

Inactivation of TRPA1 by Mg^{2+} was unexpected, given that under physiological conditions, this ion is present at millimolar concentrations inside and outside cells. If inactivation is mediated by the entry of divalent cations, then it might be predicted that physiologically relevant concentrations of intracellular Mg^{2+} would inactivate the channel. To determine whether this is the case, we measured TRPA1 currents in response to prolonged exposure to Cin in cells perfused with varying concentrations of free Mg^{2+}. Inhibition by the TRPA1-specific blocker HC-030031 (10 μM) (15) confirmed that the currents were entirely mediated by TRPA1 channels. Perfusion with 8.8 mM free Mg^{2+} strongly reduced the magnitude of the currents, whereas perfusion with 1.8 mM free Mg^{2+}, a physiologically relevant concentration, had no effect when compared with perfusion with a low concentration of free Mg^{2+} (0.35 mM; Fig. 2, *E* and *F*). Therefore, physiologically relevant resting levels of free Mg^{2+} are not expected to inactivate TRPA1. Moreover, the steep dependence of the TRPA1 currents on the intracellular Mg^{2+} concentration suggests that the process by which divalent cations speed inactivation of TRPA1 is highly cooperative.

Conventional Methods Cannot Be Used to Assign a Location for Ca^{2+} Regulation of TRPA1—Having established that potentiation and inactivation of TRPA1 are mediated by distinct processes, we next examined whether the Ca^{2+} regulation of each process was due to Ca^{2+} binding to the outside of the channel or to entry of Ca^{2+} through the channel and binding of Ca^{2+} to an intracellular target. If Ca^{2+} entry mediates either process, it might be possible to disrupt the effect of extracellular Ca^{2+} with an intracellular Ca^{2+} chelator. The preceding experiments were all performed with 5 mM EGTA, indicating that at this concentration, EGTA does not block potentiation or inactivation. Moreover, reducing the buffer to 20 μM EGTA only slightly increased the potentiation of the currents and had no effect on the rate of inactivation (-fold increase of 2.50 ± 0.29, T50 of 5.0 ± 0.5 s, n = 5; Fig. 2, *C* and *D*).

Because Ca^{2+} might act close to the site of entry, where EGTA would be ineffective, we also tested whether potentiation or inactivation of TRPA1 was affected by including the fast Ca^{2+} chelator BAPTA in the pipette. For these experiments, TRPA1 currents were activated by MO, which has a similar mechanism of action as Cin (37). The Ca^{2+}-dependent potentiation and inactivation of TRPA1 currents were not different between cells that were dialyzed with 5 mM BAPTA and those dialyzed with 20 μM EGTA (supplemental Fig. 2). In similar experiments, other groups have reported only a partial block of TRPA1 activation by BAPTA (21, 24). Therefore, either Ca^{2+} acts on the extracellular side of the channel, or the Ca^{2+} buffers at the concentrations we used were not effective in interfering with the binding of Ca^{2+} to its intracellular target. This might be the case if Ca^{2+} acts at a site very close to the permeation pathway or if the buffer is saturated by the large Ca^{2+} influx through the channels.

Mutation of a Proposed EF-hand Does Not Affect Potentiation or Inactivation—It has recently been proposed that an EF-hand located within the N terminus of TRPA1 mediates Ca^{2+} activation (20, 21). To confirm this result and determine if this site also mediates inactivation of TRPA1, we mutated each of three residues proposed to participate in activation of TRPA1 by Ca^{2+} (S471R/D472A, L475A, D480A; see supplemental Fig. 3). None of the mutations had any effect on Ca^{2+}-dependent potentiation or Ca^{2+}-dependent inactivation (supplemental

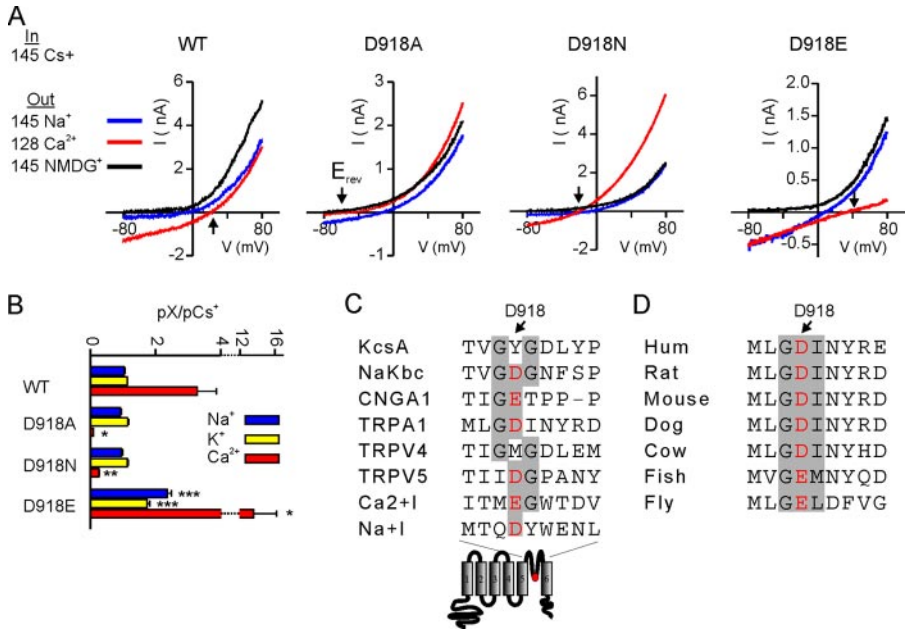

FIGURE 3. **Pore region mutations reduce Ca^{2+} permeability of TRPA1.** *A*, whole cell patch clamp recording of wild-type or mutant TRPA1 currents activated by Cin (100 μM). *Plots* show the current in response to a ramp depolarization (1 V/s) in the presence of the indicated extracellular cation (Na^+, $NMDG^+$, or Ca^{2+}). The extracellular solution was rapidly exchanged to minimize changes in the magnitude of the currents during the recording. The *arrow* indicates the reversal of the current with 128 mM Ca^{2+} in the bath. Intracellular solution was HB-Cs^+. *B*, ion selectivity was calculated based on the reversal potential of the current as measured from experiments as in *A*. D918A ($n = 3$) and D918N ($n = 6$) showed dramatically reduced Ca^{2+} permeability, whereas D918E ($n = 8$) had increased Ca^{2+} permeability as compared with wild type ($n = 6$). *C*, the S5-S6 region of TRPA1 aligned with that of related cation-permeable channels. Conserved acidic residues important for ion permeability are shown in *red*. *Gray shading* highlights the conserved GXG sequence in the selectivity filter. Note that Asp^{918} is at the same position as the Tyr in the GYG motif of the K^+ channel. Pore region alignment from multiple channels was based partly on Ref. 49. *D*, alignment of the putative selectivity filters of TRPA1 from multiple species. Data represent the mean ± S.E. Significance was determined by two-tailed Student's *t* test and was Bonferroni-corrected. *, $p < 0.05$; **, $p < 0.01$; ***, $p < 0.001$. *Ca2+I* and *Na+I*, the first transmembrane domains of the Ca^{2+} and Na^+ channel, respectively. Accession numbers are as follows: POA334 (KcsA), ZP_02523257 (NaKbc), ZP_02523257 (CNGA1), NP_997491 (TRPA1), NP_076460 (TRPV4), NP_446239 (TRPV5), Q13936 (Ca^{2+}I), NP_062139 (Na^+I), NP_015628 (human TRPA1), NP_997491 (rat TRPA1), NP_808449 (mouse TRPA1), XP_544123 (dog TRPA1), XP_581588 (cow TRPA1), NP_001007066 (fish TRPA1), NP_001097554 (fly TRPA1).

Fig. 3). Similar results were obtained with a clone of rTRPA1 that was not fused to YFP (L475A and D480A were tested; supplemental Fig. 4). To determine whether the differences between our results and those of Doerner *et al.* (21) were due to the use of different species variants of TRPA1 or to different activating chemicals, we introduced mutations into two sites on hTRPA1 (L474A and D479A) and measured potentiation following both Cin and MO activation. Mutation of Leu^{474} in hTRPA1 had no effect on Ca^{2+} potentiation following Cin or MO activation, whereas mutation of Asp^{479} abrogated channel function, as previously noted (21) (supplemental Figs. 5 and 6). Therefore, as assessed under a variety of conditions, residues in a putative EF-hand do not play a critical role in potentiation or inactivation of TRPA1, and EF-hand mutant channels cannot be used to assign a location for Ca^{2+} regulation. We noted that mutation of Asp^{480} in rTRPA1 destabilized opening of the channel by Cin, and this region, which is in close proximity to N-terminal cysteine residues that are the targets for pungent chemicals (17, 18), may therefore be more generally involved in channel gating.

A Pore Region Mutation Disrupts Ca^{2+}-dependent Potentiation and Inactivation of TRPA1—A more direct way to assess the role of Ca^{2+} entry in potentiation and inactivation of TRPA1 is to reduce the Ca^{2+} permeability of the channel and determine whether it can still be potentiated or inactivated by extracellular Ca^{2+}. In other structurally related ion channels, this has been accomplished by mutation of acidic residues in the pore region (34, 38). An alignment of TRPA1 with other cation channels places Asp^{918} in the selectivity filter at the same position as the tyrosine residue in the GYG motif of the potassium channel (39) (Fig. 3*C*). We therefore mutated Asp^{918} and characterized the ion selectivity of the Cin-activated currents by rapidly exchanging the external solution with those containing either Na^+, Cs^+, K^+, or Ca^{2+} as the only permeable cation. The reversal potential of the current under these bionic conditions can be used to calculate permeability relative to Cs^+, which was the only cation present in the pipette solution (Fig. 3*A*) (34). Consistent with previous reports (3), we found that wild-type TRPA1 channels are highly Ca^{2+}-permeable ($P_{Ca}/P_{Cs} = 3.28 \pm 0.58$, $n = 6$). Mutation of Asp^{918} to alanine (D918A) led to a reduction in calcium permeability of nearly 2 orders of magnitude ($P_{Ca}/P_{Cs} = 0.08 \pm 0.01$, $p < 0.05$; $n = 3$; Fig. 3, *A* and *B*). A charge-neutralizing substitution that did not change the size of the amino acid side chain, D918N, produced channels with an intermediate Ca^{2+} permeability ($P_{Ca}/P_{Cs} = 0.26 \pm 0.01$, $p < 0.01$; $n = 6$; Fig. 3, *A* and *B*), and the charge conserving substitution D918E increased Ca^{2+} permeability ($P_{Ca}/P_{Cs} = 13.56 \pm 2.63$, $p < 0.05$; $n = 8$; Fig. 3, *A* and *B*). Note that the *D* to *E* substitution is found in TRPA1 orthologs from several species, including zebrafish and *Drosophila* (Fig. 3*D*).

If Ca^{2+} entry mediates either potentiation or inactivation, we expected that one or both of these processes would be impaired in the D918A mutant, which is poorly permeable to Ca^{2+}. Indeed, the D918A mutant showed virtually no potentiation or inactivation in response to the addition of 2 mM Ca^{2+} following activation with Cin (-fold increase of 1.06 ± 0.02, $p < 0.001$; T50 of 105.8 ± 19.3 s, $p < 0.001$; $n = 5$; Fig. 4, *B*, *E*, and *F*). According to this logic, the D918N mutant, which has an intermediate permeability to Ca^{2+}, should show a milder deficit in potentiation and inactivation. As seen in Fig. 4, D918N currents showed robust potentiation in response to extracellular Ca^{2+} (-fold increase of 1.52 ± 0.15; $n = 5$), but potentiation was slowed and resembled the response of wild-type channels to a much lower external Ca^{2+} concentration (Fig. 4*C*; compare with Fig. 2*A*). Inactivation of D918N channels was also signifi-

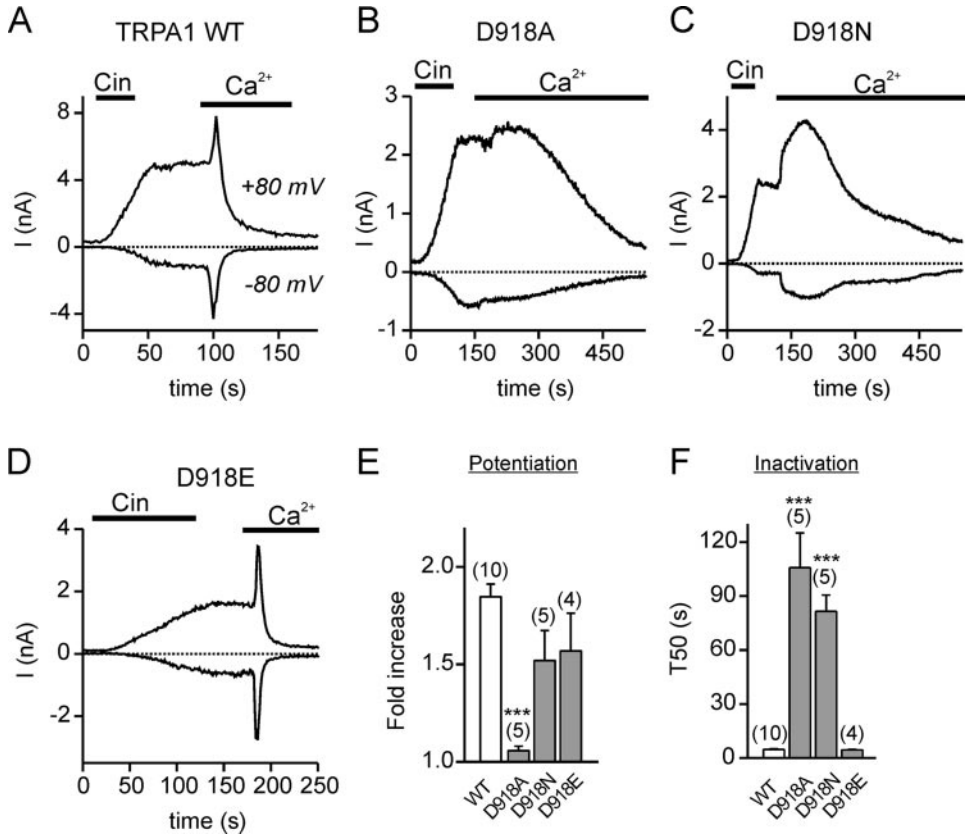

FIGURE 4. **Pore region mutations that reduce Ca^{2+} permeability disrupt Ca^{2+} potentiation and inactivation of TRPA1.** *A–D*, effect of extracellular Ca^{2+} (2 mM) on wild-type and mutant TRPA1 currents activated by brief exposure to Cin (100 μM). *B*, extracellular Ca^{2+} caused no significant potentiation and only slow inactivation of the mutant D918A, which is poorly permeable to Ca^{2+}. *C*, currents carried by the D918N mutant, which has an intermediate Ca^{2+} permeability, were strongly potentiation by Ca^{2+}, but potentiation was slowed as compared with wild type. *D*, currents carried by the D918E mutant, which has an enhanced Ca^{2+} permeability, were strongly activated and rapidly inactivated by extracellular Ca^{2+}. *E* and *F*, average data from experiments as in *A–D*, quantified as in Fig. 1. Wild-type data are reproduced from Fig. 1. Significance was determined by two-tailed Student's *t* test with Bonferroni correction for multiple samples. ***, $p < 0.001$. Internal solution was HB-Cs^+, which contained 5 mM EGTA.

cantly slowed as compared with wild type (T50 of 81.4 ± 9.2 s, $p < 0.001$; $n = 5$; Fig. 4*F*). In contrast, the response to Ca^{2+} of the highly Ca^{2+}-permeable D918E mutant was indistinguishable from that of wild-type currents (-fold increase of 1.57 ± 0.19, $p > 0.05$; T50 of 4.5 ± 0.3 s, $p > 0.05$; $n = 4$; Fig. 4, *D–F*).

To determine if the decrease in potentiation of D918A currents by Ca^{2+} could be attributed to saturation of the activation of the channels by Cin, we measured the magnitude of D918A currents following prolonged Cin exposure, which is expected to activate all available channels. Prolonged Cin exposure elicited currents of 4.1 ± 0.9 and −1.9 ± 0.7 nA at +80 and −80 mV, respectively, ($n = 6$), which was ~2 times the size of the currents used for assessing Ca^{2+} potentiation (2.1 ± 0.1 and −0.54 ± 0.07 nA at +80 and −80 mV, respectively, $n = 5$). Note that current magnitudes of all pore mutants were somewhat reduced as compared with the wild-type current, but compared with each other, they were not significantly different (2.3 ± 0.1 and −0.27 ± 0.04 nA at +80 and −80 mV, respectively, $n = 5$ for D918N; 2.4 ± 0.1 and −1.4 ± 0.9 nA at +80 and −80 mV, respectively, $n = 4$ for D918E).

Potentiation and Inactivation of TRPA1 Channels Can Be Attributed to Permeation of Ca^{2+} through the Channel—It is well recognized that permeant ions can alter the gating of ion channels, presumably because their occupancy in the permeation pathway impedes channel closure (40). It has also been shown that mutations of the pore of ion channels can affect gating (*e.g.* see Refs. 41 and 42). Indeed, the activation of the TRPA1 pore mutants was somewhat more sluggish than that of wild-type currents (Fig. 4, *A–D*); this was confirmed by measurement of the 50% activation time, which showed a 2-fold slowing for D918A currents as compared with wild-type currents (79.3 ± 6.9 s for D918A and 48.9 ± 5.4 s for wild type, $p < 0.01$, measured from experiments where Cin was applied until the currents reached saturation, as in Fig. 1*C*). It was therefore important to determine whether mutation of the TRPA1 pore disrupted potentiation and inactivation through reduced Ca^{2+} influx, as we hypothesized, or via a direct effect on the gating of the channel. If the mutation principally affected Ca^{2+} influx, we reasoned that potentiation and inactivation might be rescued by reducing the intracellular Ca^{2+} buffering so as to allow accumulation of intracellular Ca^{2+}. As shown in Fig. 5*A*, Cin-activated D918A currents were not potentiated or inactivated by 2 or 10 mM extracellular Ca^{2+} when intracellular Ca^{2+} was buffered with 5 mM EGTA (Fig. 5, *A* and *B*), and lowering the concentration of EGTA to 20 μM partially rescued both potentiation and inactivation (Fig. 5, *A* and *B*).

We confirmed that the small Ca^{2+} flux through D918A channels produced a significant elevation of intracellular Ca^{2+} under conditions of low Ca^{2+} buffering by repeating the experiment with the ratiometric Ca^{2+} indicator fura-4F in the pipette. The addition of 2 or 10 mM Ca^{2+} to the bath produced a Ca^{2+} elevation of 1–3 μM in D918A-expressing cells activated with Cin (Fig. 5, *C* and *D*). Moreover, this elevation of intracellular Ca^{2+} was blocked by including 5 mM EGTA in the pipette (Fig. 5, *C* and *D*). Interestingly, in the cells expressing wild-type channels, EGTA did not block potentiation or inactivation, and Ca^{2+} imaging revealed a substantial elevation of intracellular Ca^{2+}, despite the presence of the buffer (Fig. 5, *C* and *D*). These data confirm that potentiation and inactivation are mediated by elevation of intracellular Ca^{2+} and that mutation of Asp^{918} disrupts inactivation by reducing Ca^{2+} permeability.

TRPA1 Is Potentiated but Is Not Inactivated by Uncaging Ca^{2+}—The previous experiments indicate that the ability of extracellular Ca^{2+} to potentiate and inactivate TRPA1 requires Ca^{2+} entry. To determine if elevation of intracellular Ca^{2+} is sufficient to potentiate and inactivate TRPA1 channels, we

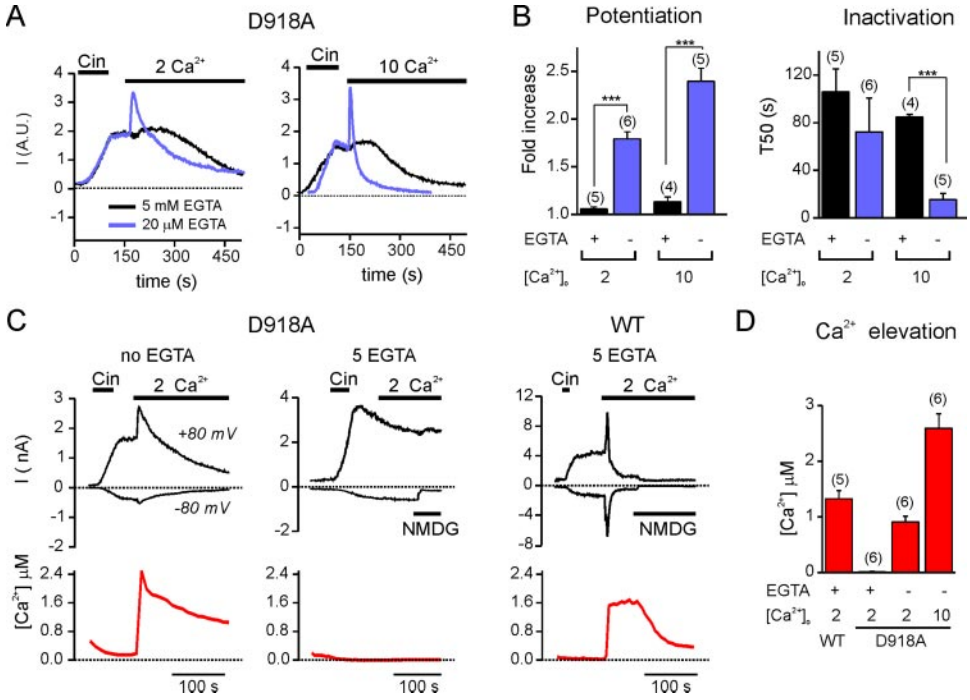

FIGURE 5. **Lowering Ca^{2+} buffering rescues potentiation and inactivation of D918A currents.** *A*, D918A currents evoked by Cin (100 μM) with 5 mM EGTA in the pipette were not potentiated or inactivated by either 2 mM (*left*) or 10 mM (*right*) extracellular Ca^{2+} (*gray lines*). Lowering the Ca^{2+} buffer in the pipette to 20 μM EGTA rescued potentiation and inactivation (*black lines*). *Traces* are from separate cells. To allow direct comparison of the currents, the responses were normalized to the amplitude of the Cin-evoked current and aligned by the time at which Ca^{2+} was added to the bath. *B*, average data from experiments as in *A*. *C*, simultaneous recordings of the current magnitude (*top*) and intracellular Ca^{2+} level (*bottom*) in D918A and wild type-expressing cells loaded through the pipette with the Ca^{2+} indicator Fura-4F (20 μM) with or without 5 mM EGTA. In the absence of intracellular Ca^{2+} buffering (no EGTA; *left trace*), D918A currents were potentiated and inactivated by bath application of 2 mM Ca^{2+}, which produced a large rise in intracellular Ca^{2+}. Including EGTA in the pipette (*middle trace*) under identical conditions eliminated the rise in intracellular Ca^{2+}, and the currents showed no potentiation or inactivation. Wild-type currents (*right trace*) supported a large Ca^{2+} influx that produced a significant elevation of intracellular Ca^{2+}, despite the presence of 5 mM EGTA in the pipette. *D*, peak intracellular Ca^{2+} concentration after the addition of extracellular Ca^{2+} from experiments as shown in *C*. In D918A-expressing cells loaded with no Ca^{2+} buffer, Ca^{2+} levels rose to the micromolar range. This elevation was completely blocked by 5 mM EGTA in the pipette. Data represent the mean ± S.E. *A.U.*, arbitrary units.

loaded cells with Ca^{2+} bound to the chelator DMNP-EDTA, which changes affinity for Ca^{2+} from 5 nM to 3 mM upon exposure to UV light (43). Fig. 6*A* shows that UV uncaging of DMNP-EDTA in the absence of extracellular Ca^{2+} caused a sustained potentiation of the Cin-activated TRPA1 current (2.70 ± 0.20-fold increase at +80 mV, $n = 5$) (Fig. 6*C*). The effect of elevating intracellular Ca^{2+} partially occluded further potentiation by extracellular Ca^{2+}, consistent with our previous observations. To confirm that the observed responses were due to elevation of intracellular Ca^{2+} and not to direct effects of the two photolytic products (44), we loaded cells with DMNP-EDTA without Ca^{2+}. Under these conditions, UV exposure caused only a slow, small increase in TRPA1 currents (Fig. 6, *B* and *C*; 1.14 ± 0.04-fold increase at +80 mV, $n = 5$), and this increase was significantly less than what we observed when DMNP-EDTA was loaded with Ca^{2+} ($p < 0.001$).

A surprising result of these experiments was that uncaging Ca^{2+} did not inactivate TRPA1 currents. This could be explained if the Ca^{2+} elevation produced by the uncaging protocol was insufficient to promote inactivation. To test this hypothesis, we compared the Ca^{2+} elevation produced by UV uncaging of DMNP-EDTA with that observed upon subsequent entry of Ca^{2+} through TRPA1 channels. Ca^{2+} levels were measured with the indicator Fluo-5F, which can be visualized with wavelengths of light that do not uncage DMNP-EDTA. Under these conditions, we found that Ca^{2+} entry produced a significantly greater global elevation of intracellular Ca^{2+} than did Ca^{2+} uncaging ($p < 0.001$; Fig. 6, *D* and *E*). It should be noted that Ca^{2+} levels at the plasma membrane upon entry through TRPA1 channels could be considerably higher than what we have measured. Together, these data indicate that elevation of intracellular Ca^{2+} by uncaging DMNP-EDTA can potentiate TRPA1 currents but not inactivate them. Inactivation may require a greater elevation of intracellular Ca^{2+} than can be achieved by Ca^{2+} uncaging.

Effect of Intracellular Ca^{2+} on TRPA1 Single Channels—To study the effects of Ca^{2+} on TRPA1 channels in more detail, we recorded the gating of single TRPA1 channels in cell-attached patches. If intracellular Ca^{2+} is sufficient to both potentiate and inactivate TRPA1 channels, the addition of extracellular Ca^{2+} to a region outside the patch pipette should potentiate and inactivate TRPA1 channels under the patch pipette. Fig. 7*A* shows a cell-attached patch clamp recording with 100 nM Ca^{2+} in the patch pipette from a TRPA1-expressing HEK 293 cell. Constitutive channel activity was observed, and this activity was increased by the addition of Cin to the bath, indicating that it represented opening of TRPA1 channels. Moreover, this activity was never observed in cells not transfected with TRPA1 (not shown). Measurement of single channel amplitudes in recordings of voltage families gave a slope conductance of 139 ± 2 pS ($n = 3$; Fig. 7*B*). Following Cin activation, the addition of Ca^{2+} to the intact cell produced dramatic potentiation, followed by a rapid decay in channel activity. Measurement of single channel currents and fitting of all points histograms indicated that the single channel conductance was unchanged in response to Cin activation or Ca^{2+} potentiation (141 ± 12 pS ($n = 3$) before Cin, 148 ± 3 pS ($n = 5$) after Cin, and 143 ± 4 pS ($n = 5$) after Ca^{2+}; Fig. 7, *C–E*). Following inactivation, sparse channel openings were observed, and these openings were of variable amplitude, possibly reflecting the sparse opening of TRPA1 channels as well as the opening of smaller endogenous Ca^{2+}-activated channels.[3] We conclude that potentiation and inactivation of TRPA1 can be

[3] Y. Y. Wang and E. R. Liman, unpublished observations.

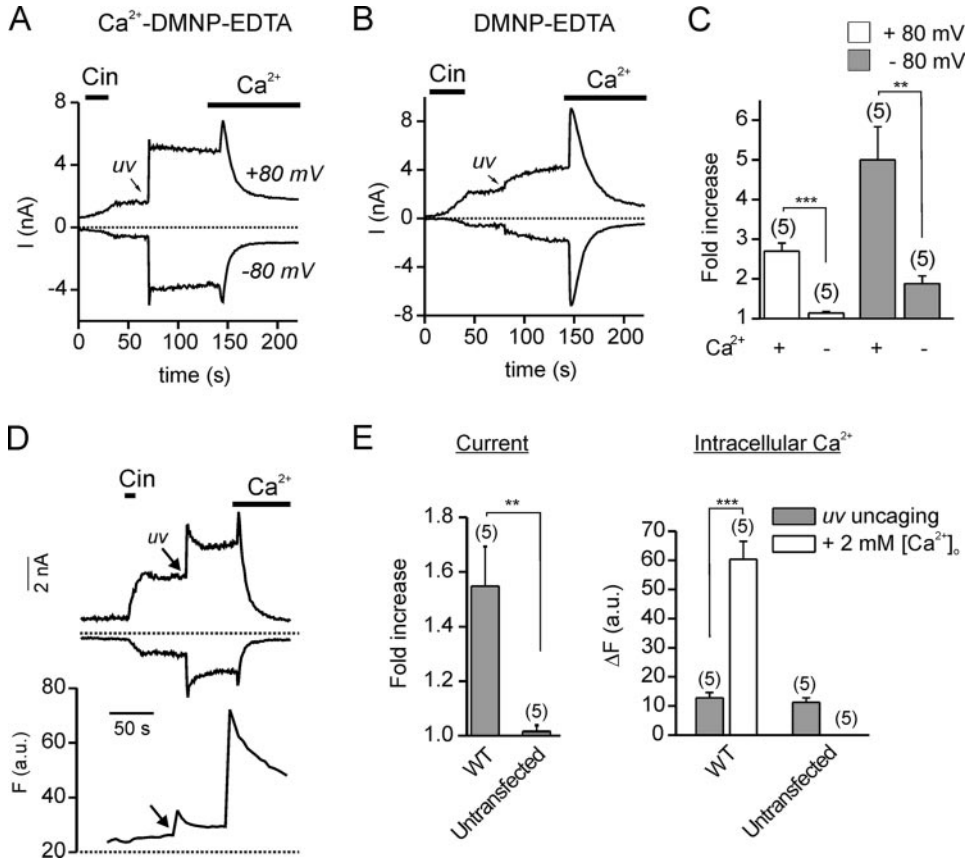

FIGURE 6. **TRPA1 currents can be potentiated by elevation of intracellular Ca^{2+} through UV uncaging of DMNP-EDTA.** *A*, potentiation of heterologously expressed TRPA1 currents in response to flash photolysis of caged Ca^{2+} (DMNP-EDTA loaded with Ca^{2+}). TRPA1 currents were activated by brief exposure to Cin (100 μM), and following stabilization of the current magnitude, UV uncaging (100 ms) potentiated the currents. Subsequent bath application of 2 mM Ca^{2+} produced nearly complete inactivation of the current. *B*, UV light had little effect on the TRPA1 currents when cells were loaded with DMNP-EDTA in the absence of intracellular Ca^{2+}. *C*, average data from experiments as in *A* and *B*. *D*, simultaneous recording of current magnitude (*top*) and intracellular Ca^{2+} (*bottom*) in HEK-293 cells expressing wild-type TRPA1 channels. The Ca^{2+} indicator Fluo-5F (10 μM) was loaded into the cells through the patch pipette. Cin (100 μM) in the absence of extracellular Ca^{2+} activated TRPA1 currents, and UV uncaging of Ca^{2+} potentiated the currents. The addition of extracellular Ca^{2+} (2 mM) caused a significantly higher Ca^{2+} elevation compared with that achieved by Ca^{2+} uncaging. *E*, mean data from experiments as in *D*. In the same experiments, the change in fluorescent emission from the Ca^{2+} indicator fluo-5F (ΔF) was measured immediately after UV uncaging and following the introduction of 2 mM Ca^{2+} to the bath. Data represent the mean ± S.E. **, $p < 0.01$; ***, $p < 0.001$. *a.u.*, arbitrary units.

induced by intracellular Ca^{2+} in a manner that is not membrane-delimited and that potentiation involves a change in channel gating and not in conductance.

Finally, we were interested in knowing whether Ca^{2+} potentiation and Ca^{2+} inactivation of TRPA1 was retained in excised patches. A technical difficulty with these experiments is that TRPA1 activity induced by MO or Cin is not preserved upon patch excision (45). Recently, it was reported that polyphosphates can restore TRPA1 activity after patch excision (45), making it now possible to study TRPA1 channels in excised patches. As shown in Fig. 8*A*, following activation by Cin and in the presence of polyP3, TRPA1 channel activity is a rapidly and reversibly potentiated by intracellular Ca^{2+}. The dose dependence of activation can be fit with the Hill equation with $K_{½}$ of 225 nM and slope of 1.8 ($n = 6$; Fig. 8*B*). We also tested whether the channels undergo inactivation under these conditions. TRPA1 currents showed only modest decay in response to 12 μM intracellular Ca^{2+} (Fig. 8*C*). At higher Ca^{2+} concentrations, more substantial decay could be observed (Fig. 8, *D* and *E*). Thus, in cell-free excised patches preactivated with Cin, TRPA1 current can be potentiated and inactivated by cytoplasmic Ca^{2+}, and potentiation occurs at lower Ca^{2+} concentrations.

DISCUSSION

Inactivation of TRPA1 can rapidly terminate signaling and therefore may be one of the key mechanisms that limit sensory activation by painful or irritating substances. Previous work has demonstrated that extracellular Ca^{2+} both potentiates and inactivates TRPA1 (4, 24). In this study, we show that inactivation of TRPA1 is not coupled to potentiation and that both processes are mediated by elevation of intracellular Ca^{2+}. In addition to these findings, we have discovered a key residue in TRPA1 that controls Ca^{2+} permeability of the channel, providing experimental evidence that the S5-S6 linker of this channel forms part of the pore region. Together, these results give insights into the mechanisms of regulation of TRPA1 and provide tools for future research.

Identification of the Ion Selectivity Filter in TRPA1—An important outcome of our work is the identification of an amino acid residue that determines Ca^{2+} selectivity of TRPA1. Ca^{2+} influx through TRPA1 undoubtedly plays an important role in the physiology and pathophysiology of sensory neurons, possibly mediating local release of inflammatory mediators as well as generating cross-desensitization of co-expressed TRPV1 channels (46).

The architectural similarity between TRP channels and voltage-gated ion channels suggests that the pore (P) region in TRP channels will be formed from the S5-S6 linker as it is in K^+ channels (39, 47). Within the P region, a "selectivity filter" is formed in the K^+ channel by a short sequence of highly conserved amino acids, with the motif TVGYG, the backbone carbonyls of which form a series of binding sites for ions within the permeation pathway (47). Recent studies suggest that the pore of Ca^{2+}- and Na^+-selective ion channels is structurally similar to that of K^+ channels (48, 49). The reported crystal structure of NaKbc, a nonselective cation channel from bacteria that shares homology with cyclic nucleotide-gated ion channels, shows that the carboxyl groups of conserved acidic residues do not

line the permeation pathway, as previously assumed, and are instead tangential to it, acting through electrostatic interactions to stabilize permeating divalent cations (48, 50).

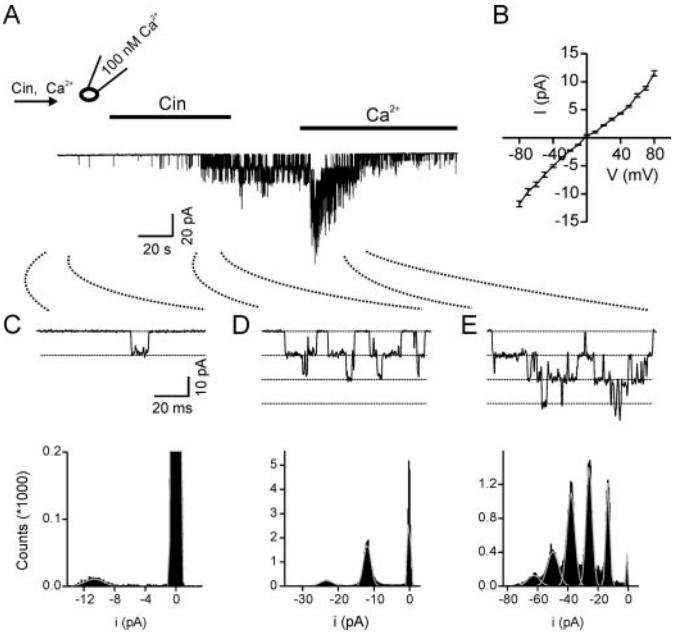

FIGURE 7. **Potentiation and inactivation of TRPA1 channels by extracellular Ca^{2+} in cell-attached patches.** *A*, TRPA1 channel activity in cell-attached patch clamp recording ($V_m = -80$ mV) in response to the addition of agonists outside the patch. *B*, conductance of spontaneously active channels measured from step depolarizations prior to exposure to Cin. The slope conductance was 139 ± 2 pS ($n = 3$). *C–E*, single channel activity at an expanded time scale (*top panel*) before and after bath application of Cin (100 μM) and following the subsequent addition of 2 mM Ca^{2+}. All points histograms (*bottom panel*) fitted with Gaussians (*gray line*) indicate that the single channel conductance was not altered upon activation by Cin or potentiation by Ca^{2+}. The pipette solution was HB-Cs^+, which contained 5 mM EGTA and 100 nM Ca^{2+}.

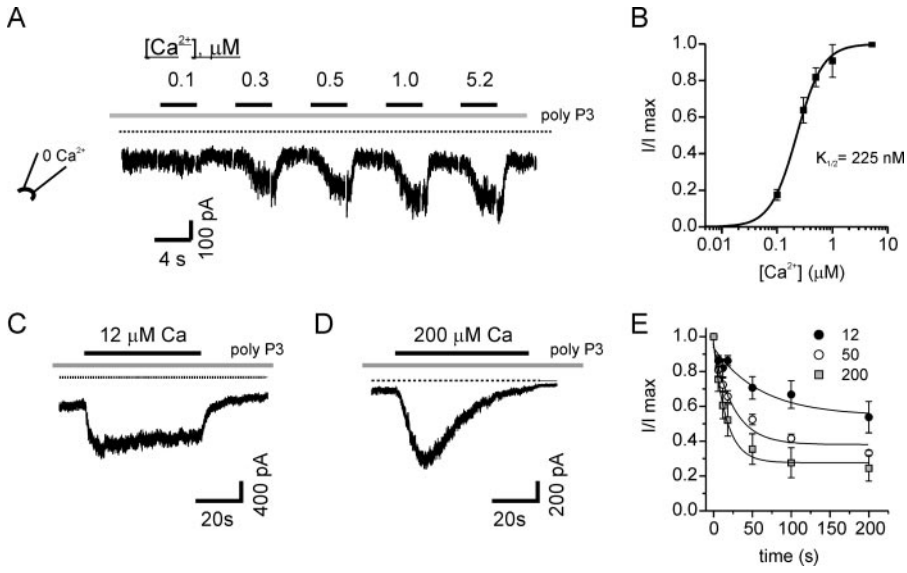

FIGURE 8. **Ca^{2+} potentiates and inactivates TRPA1 channels in excised patches.** *A*, current activation ($V_m = -80$ mV) in response to increasing concentrations of Ca^{2+} in inside-out patches from TRPA1-expressing HEK-293 cells. Currents were activated by brief exposure to Cin (100 μM) in cell-attached recording mode, and all measurements from excised patches were obtained in the presence of polyP3 (1 mM). *B*, average Ca^{2+} dose-response curve from experiments as shown in *A* (data were normalized to the peak current in each patch). Fit was with $V_{max} = 1$, $K_{1/2} = 0.225$ μM, $n = 1.83$. Data are represented by the mean ± S.E., $n = 6$. *C* and *D*, currents activated by 12 μM Ca^{2+} (*C*) or 200 μM Ca^{2+} (*D*) applied to the cytoplasmic side of inside-out patches ($V_m = -80$ mV). *E*, average data for the rate of current decay from experiments as in *C* and *D*. At lower cytoplasmic Ca^{2+} concentrations, the currents decayed more slowly. Data are represented by the mean ± S.E., $n = 4–5$.

An alignment of TRPA1 with NaKbc and KcsA shows that Asp^{918}, which we have identified as a key determinant of the Ca^{2+} permeability of TRPA1, aligns with the acidic residue in NaKbc that stabilizes permeating Ca^{2+} and with the tyrosine in the K^+ channel that is essential for K^+ selectivity (Fig. 2*C*). It also aligns with a methionine in TRPV4 and an aspartate in TRPV5, which are key determinants of ion selectivity in these channels (51, 52), and it is near an aspartate in *Drosophila* TRP that has been shown to determine ion selectivity *in vivo* (38). Mutation of Asp^{918} to Ala nearly eliminated Ca^{2+} permeability of the channel, whereas substitution with the size-conserving uncharged Asn residue caused a more moderate decrease in Ca^{2+} permeability, and substitution with the charge-conserving larger Glu residue led to an increase in Ca^{2+} permeability. These results are inconsistent with a direct coordination of Ca^{2+} by Asp^{918} within the constrained environment of the ion permeation pathway and instead indicate that Asp^{918} stabilizes the permeating Ca^{2+} ions at a distance by electrostatics, like the stabilization of Ca^{2+} by acidic residues in the pore of the NaKbc channel (48, 50).

Potentiation of TRPA1 by Intracellular Ca^{2+}—Our data support and extend previous observations that TRPA1 channels can be activated by elevation of intracellular Ca^{2+} (20, 21, 23). Gating of TRPA1 by intracellular Ca^{2+} may be the mechanism by which TRPA1 is activated downstream of bradykinin and other inflammatory mediators that bind to G protein-coupled receptors, although a role for other signaling molecules has also been proposed (8, 9, 53). Activation of TRPA1 has been observed in response to intracellular dialysis of Ca^{2+}, with half-activation concentrations of 900 nM and 6 μM measured by two different groups (20, 21). Activation of TRPA1 by intracellular Ca^{2+} has also been observed in excised patches (20, 21), but recent data indicate that a co-factor lost upon patch excision is required to maintain these responses (23, 45). In the presence of polyP3, which restores TRPA1 activity (45), we found that TRPA1 channels could be activated at concentrations of Ca^{2+} just slightly higher than the resting level ($K_{½}$ ~225 nM); this is in contrast to two other Ca^{2+}-activated TRP channels, TRPM4 and TRPM5, which in excised patches require micromolar concentrations of Ca^{2+} to be activated (27, 30, 54–57).

By studying the D918A TRPA1 channel, in which Ca^{2+} permeability is reduced, we provide evidence that potentiation of TRPA1 by extracellular Ca^{2+} is mediated by Ca^{2+} entry. Importantly, Ca^{2+} potentiation of D918A currents was blocked by including 5 mM EGTA in the pipette and could be restored by lowering the concentration of EGTA. In addition to demonstrat-

ing that intracellular Ca^{2+} potentiates TRPA1, these data suggest that, under some conditions, TRPA1 channels can respond to a global change in the intracellular Ca^{2+} concentration (58). This was further confirmed by our observation that TRPA1 channels in cell-attached patches could be potentiated by the addition of Ca^{2+} to a region outside of the patch. Similar results were recently reported for activation of TRPA1 in the absence of a pungent chemical (23). We noted that potentiation was accompanied by an increase in channel activity, without a change in channel conductance. A previous report showing a decrease in channel conductance during potentiation may be attributed to a concomitant block of the channel by extracellular Ca^{2+} (24).

Our report is also the first to show that TRPA1 can be potentiated by elevation of intracellular Ca^{2+} through UV uncaging of the Ca^{2+} cage DMNP-EDTA. This method has been extensively used in assessing the role of Ca^{2+} signaling in synaptic transmission and vesicle release as well as for studying Ca^{2+} regulation of ion channels, including TRP channels (33, 43–45, 57, 59). In studying TRPA1, which can be modified by a number of reactive compounds, it was important to establish that the effects of uncaging could not be attributed to effects of the two iminodiacetic acids generated by the photolysis of DMNP-EDTA (43, 44). Our observation that UV uncaging of DMNP-EDTA in the absence of intracellular Ca^{2+} caused only a small, slow increase of the TRPA1 currents indicates that the potentiation of TRPA1 currents upon UV uncaging of DMNP-EDTA could be largely attributed to Ca^{2+} elevation. Therefore, with the proper controls, flash photolysis of DMNP-EDTA is a useful method for studying Ca^{2+} activation of TRPA1. Interestingly, with this method, we observed a long lasting potentiation of TRPA1, which was not accompanied by inactivation. In similar experiments with other Ca^{2+}-activated TRP channels, a transient activation of the currents was observed, consistent with the observed transient elevation of Ca^{2+} (33, 57). The absence of inactivation could be explained if UV uncaging of DMNP-EDTA did not produce sufficiently high intracellular Ca^{2+} levels. This interpretation is supported by our observation that the Ca^{2+} levels attained by UV uncaging of DMNP-EDTA were significantly lower than those attained through entry of Ca^{2+} through TRPA1 channels.

Intracellular Ca^{2+} Elevation Mediates Inactivation of TRPA1—Inactivation of heterologously expressed TRPA1 by extracellular Ca^{2+} has been well documented (3, 4, 8, 19, 20, 24) and is also observed in neurons (*e.g.* see Ref. 12). Our results show that, like potentiation, inactivation by extracellular Ca^{2+} requires Ca^{2+} entry. Thus D918A channels, which are poorly permeable to Ca^{2+}, inactivate only slowly in response to extracellular Ca^{2+}, and inactivation can be largely restored by lowering intracellular Ca^{2+} buffering. Moreover, TRPA1 channels in excised and cell-attached patches could be inactivated through elevation of intracellular Ca^{2+}, in the absence of extracellular Ca^{2+}. It is perhaps not surprising that elevation of intracellular Ca^{2+} mediates inactivation of TRPA1, since it induces inactivation/desensitization of many ion channels and receptors, including both Ca^{2+}-permeable and Ca^{2+}-impermeable TRP channels (25–31, 60).

Given that intracellular Ca^{2+} potentiates and inactivates TRPA1, is there a mechanism that ensures that potentiation precedes inactivation? In voltage-gated Na^+ and K^+ channels, inactivation is coupled to voltage-dependent activation, such that the channels first open and then inactivate (61). A similar coupling between Ca^{2+}-dependent activation/potentiation and inactivation of TRPA1 appears unlikely for several reasons. First, in response to moderate elevation of intracellular Ca^{2+} by UV uncaging of DMNP-EDTA, potentiation can be observed in the absence of inactivation, indicating that the two processes are not strictly coupled. Moreover, inactivation can be induced by extracellular Mg^{2+} in the absence of potentiation, suggesting that the two processes are mediated by intracellular signaling events with different ionic specificities. Excised patch recording suggests that inactivation follows potentiation because inactivation is relatively slow at the low Ca^{2+} concentrations that maximally activate the channel. Moreover, these data predict that a modest Ca^{2+} elevation in response to signaling by G protein-coupled receptors or receptor tyrosine kinases might activate without inactivating TRPA1. The subsequent entry of Ca^{2+} through TRPA1 channels may then terminate the signal.

Where is the Site for Ca^{2+} Potentiation and Inactivation of TRPA1?—An attractive hypothesis is that Ca^{2+} activates TRPA1 by binding directly to a putative EF-hand on the N terminus of TRPA1, as proposed recently by two groups (20, 21). Within the stretch of 12 amino acids that comprise the Ca^{2+} binding site on a canonical EF-hand, 6 residues coordinate Ca^{2+} (62). Doerner *et al.* (21) found that of these sites, mutations of only one (Leu^{474}) significantly reduced Ca^{2+} activation of the channels. This is surprising in that Leu^{474} occupies a position that contributes a backbone carbonyl to the Ca^{2+} binding site of a canonical EF-hand, and Leu is not commonly observed at this position (62). Zurborg *et al.* (20) found, in contrast, that mutant channels with charge-neutralizing substitutions of the acidic residues that flank the EF-hand were no longer sensitive to Ca^{2+}, as assayed by intracellular Ca^{2+} dialysis and other methods. Our experiments show that neither Leu^{474} nor Asp^{479} is necessary for Ca^{2+} potentiation of TRPA1. We observed robust potentiation of hTRPA1 L474A and of rTRPA1 L475A (analogous to L474A in hTRPA1), using both a fusion protein with YFP and the unfused channel. The absence of potentiation of hTRPA1 L474A currents in the experiments by Doerner *et al.* (21) could be due to a saturation of the response to the agonist (MO), which can occlude activation by Ca^{2+} (supplemental Fig. 6). In agreement with Doerner *et al.* (21) and contrary to the report by Zurborg *et al.* (20), we found that the D479A mutation of hTRPA1 abrogated channel activity. The equivalent mutation in rTRPA1, D480A, did not interfere with Ca^{2+} potentiation but appeared to destabilize channel activation. Together, these results make it unlikely that an N-terminal region proposed to form an EF-hand contributes to Ca^{2+} potentiation of TRPA1, although it may otherwise regulate gating of TRPA1.

Other mechanisms by which Ca^{2+} could potentiate or inactivate TRPA1 include direct binding to other acidic residues on the intracellular side of TRPA1, of which there are more than 100, or binding to other proteins that regulate TRPA1 either

directly or indirectly. A prime suspect for the calcium sensor is calmodulin, which mediates the Ca^{2+}-dependent facilitation and inactivation of voltage-gated Ca^{2+} channels (63–68) and desensitization of Ca^{2+}-permeable cyclic nucleotide-gated ion channels (69, 70) and which binds to several TRP channels (71–76). However, expression of TRPA1 with a dominant negative form of calmodulin did not abrogate Ca^{2+} potentiation or inactivation (20), suggesting that calmodulin is unlikely to be the sensor for Ca^{2+} regulation of TRPA1.[3] Alternatively, elevation of intracellular Ca^{2+} could activate enzymatic processes that modulate channel activity. Other TRP channels are regulated by $PI(4,5)P_2$, which can be depleted by elevation of intracellular Ca^{2+} (77). Depletion of $PI(4,5)P_2$ underlies desensitization of TRPV1, TRPM4, TRPM5, TRPM7, and TRPM8 (27–31, 78–80). $PI(4,5)P_2$ depletion has also been proposed to underlie sensitization of TRPV1 in response to the proalgesic agents bradykinin and nerve growth factor that activate receptors coupled to phospholipase C (81, 82). A role for $PI(4,5)P_2$ depletion in the desensitization of TRPA1 is supported by recent experiments showing that cross-desensitization of MO-evoked currents in sensory neurons by capsaicin, acting on TRPV1, can be blocked by infusion of $PI(4,5)P_2$ through the pipette (19) and by evidence that $PI(4,5)P_2$ can restore channel activation following partial, but not complete, inactivation in excised patches (83). But other data suggest that $PI(4,5)P_2$ depletion contributes to activation or sensitization of TRPA1 (9, 53). Using newly developed methods for manipulating $PI(4,5)P_2$ levels (79, 84), we found that $PI(4,5)P_2$ depletion neither activates nor inactivates TRPA1 (see supplemental Fig. 7), although we cannot rule out the possibility that changes in $PI(4,5)P_2$ levels might have more subtle effects on channel function. Yet another mechanism by which Ca^{2+} regulates TRP channels is through Ca^{2+}-activated phosphatase calcineurin (85), although a recent report does not support a role for calcineurin in desensitization of TRPA1 (19).

Ca^{2+} Regulation of TRPA1 in Sensory Neurons—In sensory neurons, intracellular Ca^{2+} can be elevated through several distinct mechanisms, each of which could affect the gating of TRPA1. For example, inflammatory mediators, such as bradykinin, can act on cognate G protein-coupled receptors to release intracellular Ca^{2+}; thermal and chemical stimuli can cause entry of Ca^{2+} through TRPV1 or TRPA1 channels; and depolarization can activate voltage-gated Ca^{2+} channels (86, 87). How elevation of Ca^{2+} contributes to activation and inactivation of TRPA1 in sensory neurons is not well understood and may require a better understanding of the complex spatial and temporal dynamics of Ca^{2+} signaling in these cells. An example of this complexity is the surprising observation that targeted deletion of either TRPA1 or TRPV1 eliminates bradykinin-evoked Ca^{2+} entry in sensory neurons (5). This suggests that the Ca^{2+} release that is evoked by bradykinin is insufficient to activate TRPA1 and that concurrent entry of Ca^{2+} through TRPV1 may be necessary. Adding to this complexity is the possibility that changes in other signaling molecules, such as depletion of $PI(4,5)P_2$, also contribute to activation of TRPA1 in sensory neurons (9, 22). A similar complexity applies to inactivation (or desensitization) of TRPA1 in sensory neurons. In behavioral studies, responses to MO show both homologous desensitization and cross-desensitization by TRPV1 activation (88, 89). Recent data indicate that the cross-desensitization of MO responses is Ca^{2+}-dependent (46) and therefore may be mediated by the mechanism we and others observe in heterologous cells. However, homologous desensitization of MO responses in sensory neurons is reported to be Ca^{2+}-independent (46) and may be mediated instead by TRPV1-dependent internalization (19). The absence of Ca^{2+}-sensitive homologous desensitization may reflect the lower current density of TRPA1 in sensory neurons (*e.g.* see Ref. 4) or differences between native and expressed channels in subunit composition or post-translational modification. Clearly, additional studies are needed to understand the complex regulation of TRPA1 in native cells.

Acknowledgments—We thank Don Arnold and Robert Chow for helpful discussions and the following individuals for generously sharing reagents: D. Julius (rTRPA1), T. Meyer (CFP-FKBP-Inp54p, Lyn_{11}-FRB), and A. Patapoutian (hTRPA1).

REFERENCES

1. Moran, M. M., Xu, H., and Clapham, D. E. (2004) *Curr. Opin. Neurobiol.* **14,** 362–369
2. Caterina, M. J., and Julius, D. (2001) *Annu. Rev. Neurosci.* **24,** 487–517
3. Story, G. M., Peier, A. M., Reeve, A. J., Eid, S. R., Mosbacher, J., Hricik, T. R., Earley, T. J., Hergarden, A. C., Andersson, D. A., Hwang, S. W., McIntyre, P., Jegla, T., Bevan, S., and Patapoutian, A. (2003) *Cell* **112,** 819–829
4. Jordt, S. E., Bautista, D. M., Chuang, H. H., McKemy, D. D., Zygmunt, P. M., Hogestatt, E. D., Meng, I. D., and Julius, D. (2004) *Nature* **427,** 260–265
5. Bautista, D. M., Jordt, S. E., Nikai, T., Tsuruda, P. R., Read, A. J., Poblete, J., Yamoah, E. N., Basbaum, A. I., and Julius, D. (2006) *Cell* **124,** 1269–1282
6. Kwan, K. Y., Allchorne, A. J., Vollrath, M. A., Christensen, A. P., Zhang, D. S., Woolf, C. J., and Corey, D. P. (2006) *Neuron* **50,** 277–289
7. Macpherson, L. J., Xiao, B., Kwan, K. Y., Petrus, M. J., Dubin, A. E., Hwang, S., Cravatt, B., Corey, D. P., and Patapoutian, A. (2007) *J. Neurosci.* **27,** 11412–11415
8. Bandell, M., Story, G. M., Hwang, S. W., Viswanath, V., Eid, S. R., Petrus, M. J., Earley, T. J., and Patapoutian, A. (2004) *Neuron* **41,** 849–857
9. Dai, Y., Wang, S., Tominaga, M., Yamamoto, S., Fukuoka, T., Higashi, T., Kobayashi, K., Obata, K., Yamanaka, H., and Noguchi, K. (2007) *J. Clin. Invest.* **117,** 1979–1987
10. Bautista, D. M., Movahed, P., Hinman, A., Axelsson, H. E., Sterner, O., Hogestatt, E. D., Julius, D., Jordt, S. E., and Zygmunt, P. M. (2005) *Proc. Natl. Acad. Sci. U. S. A.* **102,** 12248–12252
11. Lee, S. P., Buber, M. T., Yang, Q., Cerne, R., Cortes, R. Y., Sprous, D. G., and Bryant, R. W. (2008) *Br. J. Pharmacol.* **153,** 1739–1749
12. Andersson, D. A., Gentry, C., Moss, S., and Bevan, S. (2008) *J. Neurosci.* **28,** 2485–2494
13. Sawada, Y., Hosokawa, H., Matsumura, K., and Kobayashi, S. (2008) *Eur. J. Neurosci.* **27,** 1131–1142
14. Xu, H., Delling, M., Jun, J. C., and Clapham, D. E. (2006) *Nat. Neurosci.* **9,** 628–635
15. McNamara, C. R., Mandel-Brehm, J., Bautista, D. M., Siemens, J., Deranian, K. L., Zhao, M., Hayward, N. J., Chong, J. A., Julius, D., Moran, M. M., and Fanger, C. M. (2007) *Proc. Natl. Acad. Sci. U. S. A.* **104,** 13525–13530
16. Bessac, B. F., Sivula, M., von Hehn, C. A., Escalera, J., Cohn, L., and Jordt, S. E. (2008) *J. Clin. Invest.* **118,** 1899–1910
17. Hinman, A., Chuang, H. H., Bautista, D. M., and Julius, D. (2006) *Proc. Natl. Acad. Sci. U. S. A.* **103,** 19564–19568
18. Macpherson, L. J., Dubin, A. E., Evans, M. J., Marr, F., Schultz, P. G., Cravatt, B. F., and Patapoutian, A. (2007) *Nature* **445,** 541–545
19. Akopian, A. N., Ruparel, N. B., Jeske, N. A., and Hargreaves, K. M. (2007) *J. Physiol.* **583,** 175–193

20. Zurborg, S., Yurgionas, B., Jira, J. A., Caspani, O., and Heppenstall, P. A. (2007) *Nat. Neurosci.* **10,** 277–279
21. Doerner, J. F., Gisselmann, G., Hatt, H., and Wetzel, C. H. (2007) *J. Biol. Chem.* **282,** 13180–13189
22. Wang, S., Dai, Y., Fukuoka, T., Yamanaka, H., Kobayashi, K., Obata, K., Cui, X., Tominaga, M., and Noguchi, K. (2008) *Brain* **131,** 1241–1251
23. Cavanaugh, E. J., Simkin, D., and Kim, D. (2008) *Neuroscience* **154,** 1467–1476
24. Nagata, K., Duggan, A., Kumar, G., and Garcia-Anoveros, J. (2005) *J. Neurosci.* **25,** 4052–4061
25. Cholewinski, A., Burgess, G. M., and Bevan, S. (1993) *Neuroscience* **55,** 1015–1023
26. Docherty, R. J., Yeats, J. C., Bevan, S., and Boddeke, H. W. (1996) *Pflugers Arch.* **431,** 828–837
27. Liu, D., and Liman, E. R. (2003) *Proc. Natl. Acad. Sci. U. S. A.* **100,** 15160–15165
28. Liu, B., Zhang, C., and Qin, F. (2005) *J. Neurosci.* **25,** 4835–4843
29. Rohacs, T., Lopes, C. M., Michailidis, I., and Logothetis, D. E. (2005) *Nat. Neurosci.* **8,** 626–634
30. Zhang, Z., Okawa, H., Wang, Y., and Liman, E. R. (2005) *J. Biol. Chem.* **280,** 39185–39192
31. Nilius, B., Mahieu, F., Prenen, J., Janssens, A., Owsianik, G., Vennekens, R., and Voets, T. (2006) *EMBO J.* **25,** 467–478
32. Aldrich, R. W., Corey, D. P., and Stevens, C. F. (1983) *Nature* **306,** 436–441
33. Zhang, Z., Zhao, Z., Margolskee, R., and Liman, E. (2007) *J. Neurosci.* **27,** 5777–5786
34. Owsianik, G., Talavera, K., Voets, T., and Nilius, B. (2006) *Annu. Rev. Physiol.* **68,** 685–717
35. Nilius, B., Talavera, K., Owsianik, G., Prenen, J., Droogmans, G., and Voets, T. (2005) *J. Physiol.* **567,** 35–44
36. Karashima, Y., Damann, N., Prenen, J., Talavera, K., Segal, A., Voets, T., and Nilius, B. (2007) *J. Neurosci.* **27,** 9874–9884
37. Bandell, M., Macpherson, L. J., and Patapoutian, A. (2007) *Curr. Opin. Neurobiol.* **17,** 490–497
38. Liu, C. H., Wang, T., Postma, M., Obukhov, A. G., Montell, C., and Hardie, R. C. (2007) *J. Neurosci.* **27,** 604–615
39. Heginbotham, L., Abramson, T., and MacKinnon, R. (1992) *Science* **258,** 1152–1155
40. Swenson, R. P., Jr., and Armstrong, C. M. (1981) *Nature* **291,** 427–429
41. Susankova, K., Ettrich, R., Vyklicky, L., Teisinger, J., and Vlachova, V. (2007) *J. Neurosci.* **27,** 7578–7585
42. Myers, B. R., Bohlen, C. J., and Julius, D. (2008) *Neuron* **58,** 362–373
43. Delaney, K. R., and Zucker, R. S. (1990) *J. Physiol.* **426,** 473–498
44. Kaplan, J. H., and Ellis-Davies, G. C. (1988) *Proc. Natl. Acad. Sci. U. S. A.* **85,** 6571–6575
45. Kim, D., and Cavanaugh, E. J. (2007) *J. Neurosci.* **27,** 6500–6509
46. Ruparel, N. B., Patwardhan, A. M., Akopian, A. N., and Hargreaves, K. M. (2008) *Pain* **135,** 271–279
47. Doyle, D. A., Morais Cabral, J., Pfuetzner, R. A., Kuo, A., Gulbis, J. M., Cohen, S. L., Chait, B. T., and MacKinnon, R. (1998) *Science* **280,** 69–77
48. Shi, N., Ye, S., Alam, A., Chen, L., and Jiang, Y. (2006) *Nature* **440,** 570–574
49. Zagotta, W. N. (2006) *Nature* **440,** 427–429
50. Alam, A., Shi, N., and Jiang, Y. (2007) *Proc. Natl. Acad. Sci. U. S. A.* **104,** 15334–15339
51. Nilius, B., Vennekens, R., Prenen, J., Hoenderop, J. G., Droogmans, G., and Bindels, R. J. (2001) *J. Biol. Chem.* **276,** 1020–1025
52. Garcia-Martinez, C., Morenilla-Palao, C., Planells-Cases, R., Merino, J. M., and Ferrer-Montiel, A. (2000) *J. Biol. Chem.* **275,** 32552–32558
53. Kim, D., Cavanaugh, E., and Simkin, D. (2008) *Am. J. Physiol. Cell Physiol.* **295,** C92–C99
54. Launay, P., Fleig, A., Perraud, A. L., Scharenberg, A. M., Penner, R., and Kinet, J. P. (2002) *Cell* **109,** 397–407
55. Hofmann, T., Chubanov, V., Gudermann, T., and Montell, C. (2003) *Curr. Biol.* **13,** 1153–1158
56. Prawitt, D., Monteilh-Zoller, M. K., Brixel, L., Spangenberg, C., Zabel, B., Fleig, A., and Penner, R. (2003) *Proc. Natl. Acad. Sci. U. S. A.* **100,** 15166–15171
57. Ullrich, N. D., Voets, T., Prenen, J., Vennekens, R., Talavera, K., Droogmans, G., and Nilius, B. (2005) *Cell Calcium* **37,** 267–278
58. Neher, E. (1998) *Neuron* **20,** 389–399
59. Neher, E., and Zucker, R. S. (1993) *Neuron* **10,** 21–30
60. Xiao, R., Tang, J., Wang, C., Colton, C. K., Tian, J., and Zhu, M. X. (2008) *J. Biol. Chem.* **283,** 6162–6174
61. Hille, B. (2001) *Ionic Channels of Excitable Membranes*, Sinauer Associates Inc., Sunderland, MA
62. Gifford, J. L., Walsh, M. P., and Vogel, H. J. (2007) *Biochem. J.* **405,** 199–221
63. Peterson, B. Z., DeMaria, C. D., Adelman, J. P., and Yue, D. T. (1999) *Neuron* **22,** 549–558
64. Lee, A., Wong, S. T., Gallagher, D., Li, B., Storm, D. R., Scheuer, T., and Catterall, W. A. (1999) *Nature* **399,** 155–159
65. Zuhlke, R. D., Pitt, G. S., Deisseroth, K., Tsien, R. W., and Reuter, H. (1999) *Nature* **399,** 159–162
66. Qin, N., Olcese, R., Bransby, M., Lin, T., and Birnbaumer, L. (1999) *Proc. Natl. Acad. Sci. U. S. A.* **96,** 2435–2438
67. DeMaria, C. D., Soong, T. W., Alseikhan, B. A., Alvania, R. S., and Yue, D. T. (2001) *Nature* **411,** 484–489
68. Liang, H., DeMaria, C. D., Erickson, M. G., Mori, M. X., Alseikhan, B. A., and Yue, D. T. (2003) *Neuron* **39,** 951–960
69. Chen, T. Y., and Yau, K. W. (1994) *Nature* **368,** 545–548
70. Bradley, J., Reisert, J., and Frings, S. (2005) *Curr. Opin. Neurobiol.* **15,** 343–349
71. Niemeyer, B. A., Bergs, C., Wissenbach, U., Flockerzi, V., and Trost, C. (2001) *Proc. Natl. Acad. Sci. U. S. A.* **98,** 3600–3605
72. Zhu, M. X., and Tang, J. (2004) *Novartis Found. Symp.* **258,** 44–58; discussion 58–62, 98–102, 263–106
73. Ordaz, B., Tang, J., Xiao, R., Salgado, A., Sampieri, A., Zhu, M. X., and Vaca, L. (2005) *J. Biol. Chem.* **280,** 30788–30796
74. Lambers, T. T., Weidema, A. F., Nilius, B., Hoenderop, J. G., and Bindels, R. J. (2004) *J. Biol. Chem.* **279,** 28855–28861
75. Kwon, Y., Hofmann, T., and Montell, C. (2007) *Mol. Cell* **25,** 491–503
76. Lishko, P. V., Procko, E., Jin, X., Phelps, C. B., and Gaudet, R. (2007) *Neuron* **54,** 905–918
77. Suh, B. C., and Hille, B. (2005) *Curr. Opin. Neurobiol.* **15,** 370–378
78. Runnels, L. W., Yue, L., and Clapham, D. E. (2002) *Nat. Cell Biol.* **4,** 329–336
79. Varnai, P., Thyagarajan, B., Rohacs, T., and Balla, T. (2006) *J. Cell Biol.* **175,** 377–382
80. Thyagarajan, B., Lukacs, V., and Rohacs, T. (2008) *J. Biol. Chem.* **283,** 14980–14987
81. Chuang, H. H., Prescott, E. D., Kong, H., Shields, S., Jordt, S. E., Basbaum, A. I., Chao, M. V., and Julius, D. (2001) *Nature* **411,** 957–962
82. Prescott, E. D., and Julius, D. (2003) *Science* **300,** 1284–1288
83. Karashima, Y., Prenen, J., Meseguer, V., Owsianik, G., Voets, T., and Nilius, B. (2008) *Pflugers Arch.* **457,** 77–89
84. Suh, B. C., Inoue, T., Meyer, T., and Hille, B. (2006) *Science* **314,** 1454–1457
85. Mohapatra, D. P., and Nau, C. (2005) *J. Biol. Chem.* **280,** 13424–13432
86. Wang, H., Ehnert, C., Brenner, G. J., and Woolf, C. J. (2006) *Biol. Chem.* **387,** 11–14
87. Okuse, K. (2007) *Int. J. Biochem. Cell Biol.* **39,** 490–496
88. Brand, G., and Jacquot, L. (2002) *Chem. Senses* **27,** 593–598
89. Simons, C. T., Carstens, M. I., and Carstens, E. (2003) *Chem. Senses* **28,** 459–465